

OMAE2017-61726

A Hydrodynamic Analysis of Motion Coupling Effect of Floating Storage Tank Supported by Marine Fenders

Mengmeng Han

Department of Civil and Environmental Engineering, Faculty of Engineering, National University of Singapore

Allan Ross Magee

Department of Civil and Environmental Engineering, Faculty of Engineering, National University of Singapore

Ling Wan*

Department of Civil and Environmental Engineering, Faculty of Engineering, National University of Singapore

Jingzhe Jin**

SINTEF Ocean
Trondheim, Norway

Chien Ming Wang

Department of Civil and Environmental Engineering, Faculty of Engineering, National University of Singapore

ABSTRACT

This study concerns a new concept of floating oil storage facility, to be deployed in coastal waters, in which separate oil storage tanks float in an array, separated by a mooring fender system. In this paper, hydrodynamic properties of a single module are investigated numerically. The effects of different mooring fender parameters including fender stiffness and fender position on the coupled motions are studied. Design criteria and a design approach for the marine fender selection are proposed. Next, time-domain simulations under random waves are performed. Finite water depth effects are taken into consideration. Then a brief parametric study on sloshing phenomenon in fender-supported tanks is conducted. Results show that a carefully designed marine fender will help reduce the roll and pitch motions of the storage tank, and thus function as a stabilizer. This analysis is the basis of a global hydrodynamic response analysis for multiple tanks, including the effects of multibody hydrodynamic interactions between tanks in the future.

NOMENCLATURES

D	Diameter of the internal tank
H	Height of the tank wall
L	Side length of the outer wall
L_w	Design wave length
d	Water depth
d_n	Draft of the tank at n% filling level
r_g	Radius of Gyration of X and Y axis
f_ω	Natural frequency ratio

g_ω	Wave frequency ratio
g_{inter}	Intersection frequency
ζ	Damping ratio
μ	Mass ratio
f_r	Excitation force ratio

1. INTRODUCTION

A new concept of floating oil storage facility designed for shallow water has been brought up recently, with one key innovation being the separated oil storage tank modules, supported by marine fenders around the tank body. The initial application is for a relatively sheltered environment near the coast, but the concept can readily be extended to other cases with suitable modifications. The floating tank supported horizontally by fenders is exposed to a combined environmental loading from wave, wind and current, among which both periodic component and constant component exists. While the constant component causes a deformation on the fender and a static deviation of the tank position, the periodic component from 1st and 2nd order wave force, would excite the translational vibration of the tank. Similar as the tank movement, the reaction force provided by the fender can also be separated into static and dynamic parts. Since the tank has a large range of different drafts (determined by loading levels), the fender supporting point would have a different vertical position from the vertical centre of gravity (VCG) of the tank. Taking moments from tank VCG and the fender reaction force would inevitably provide a tilting moment to the tank, thus affecting its rotational motion. In this way the translational and rotational motion of the tank becomes coupled

* Previous affiliation: Norwegian University of Science and Technology (NTNU)
Email: ling.wan@ntnu.no

**Previous affiliation: Marintek, Norway

$$\text{IRF}(\tau) = c(\tau) * \int_0^{\infty} 4 * B(f) * \cos(2\pi f\tau) d\tau \quad (2.4)$$

Where B(f) is the frequency-dependent damping matrix, and c(τ) is the cut-off scaling function with the following form:

$$c(\tau) = \exp \left[-\left(\frac{3\tau}{T_c} \right)^2 \right] \quad (2.5)$$

Where T_c is the cut-off time.

Added mass and damping load is at each time step calculated by:

$$F(t) = -A(\infty)\ddot{x}(t) - \int_0^{\infty} \text{IRF}(\tau)\dot{x}(t - \tau)d\tau \quad (2.6)$$

The tank-fender system modelled in Orcaflex is shown below. Following the design concept, two fenders are applied at each side of the tank so that the contact force is not concentrated at one location. The stiffness of the fendering system is determined by that of the two fenders aggregating together. The fender is installed on rectangular supporting barges. Both the barges and the fenders are considered as non-moving elastic solid. The barge is modelled to be stiff, with stiffness 100 times as high as the fender, so that once the lateral movement of the tank is large enough for it to penetrate through the fender and collide into the barge, there'll be a large impact force between these two. This is an undesirable scenario and is not allowed to show up in the design.

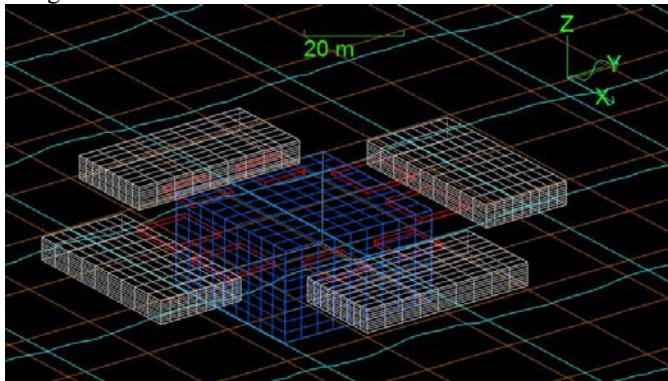


Figure 2.3 Orcaflex model of tank-fender system

3. MOTION RESPONSE OF FENDER-SUPPORTED TANKS

Based on the site condition the shallow water wave condition is applied to all the cases studied. But a brief introduction of the effect caused by shallow water is given in the end of this section. All the parameters used are summarized as follows in a dimensionless form:

D/H	1.75
L/D	1.04
L/L_w	0.50
d₀/d	0.35
d₄₀/d	0.56
d₁₀₀/d	0.88

Table 3.1 Tank Parameters

The tank has a deep draft when it's fully-loaded and the internal free surface area is quite large. These properties signify the importance of the effects of shallow water and sloshing. The effect of sloshing of the interior fluid is treated below in Section 5.

3.1 FREQUENCY DOMAIN NUMERICAL SIMULATION

In the following study, an incident wave angle of 90-degree is selected as the critical wave condition because this is when maximum translational motion takes place. Besides, out of the tank's geometric symmetry, the 0 degree and 90 degree wave responses are repetitive. A variety of fender stiffness is applied, but for the same reason stated above, the fender effect will be given by the sway natural frequencies it excites. Under this wave heading, surge, pitch and yaw motions are zero, heave motion is not influenced by the existence of marine fenders, and the remaining two DOFs, sway and roll, become the main concerns.

Due to the same reason stated above, dimensionless parameters are used to describe the frequency domain properties of motion responses. In the following sections the two parameters regarding frequency are used: $f_{\omega} = \omega_{22}/\omega_{44}$ is the natural frequency ratio, where ω_{22} and ω_{44} are respectively the natural frequencies of sway and roll; and $g_{\omega} = \omega/\omega_{44}$ is the wave frequency ratio, where ω is the wave excitation frequency. f_{ω} is essentially a dimensionless parameter of fender stiffness, and g_{ω} a dimensionless wave frequency. For the free floating body, $\omega_{22} = 0$ because there is no sway restoring force.

The motion responses of the empty and fully-loaded tanks are shown in figure 3.2 and 3.3. The response amplitudes are taken at VCG of the tank. The VCG is at +1.51 m above the waterline when tank is empty, and -7.44 m when tank is full. In a practical design the contact force cannot be exceedingly large, so fender stiffness is also restricted. As a result, all selected fender stiffness in the study gives a natural frequency ratio $f_{\omega} < 1$, to ensure the contact force is in the acceptable range. Besides, to control the maximum response, a 10% viscous damping ratio is used in all the simulation in both translational and rotational DOFs. The damping ratio will be checked against CFD simulation results and model tests in future work.

Dimensionless Tank Parameters	

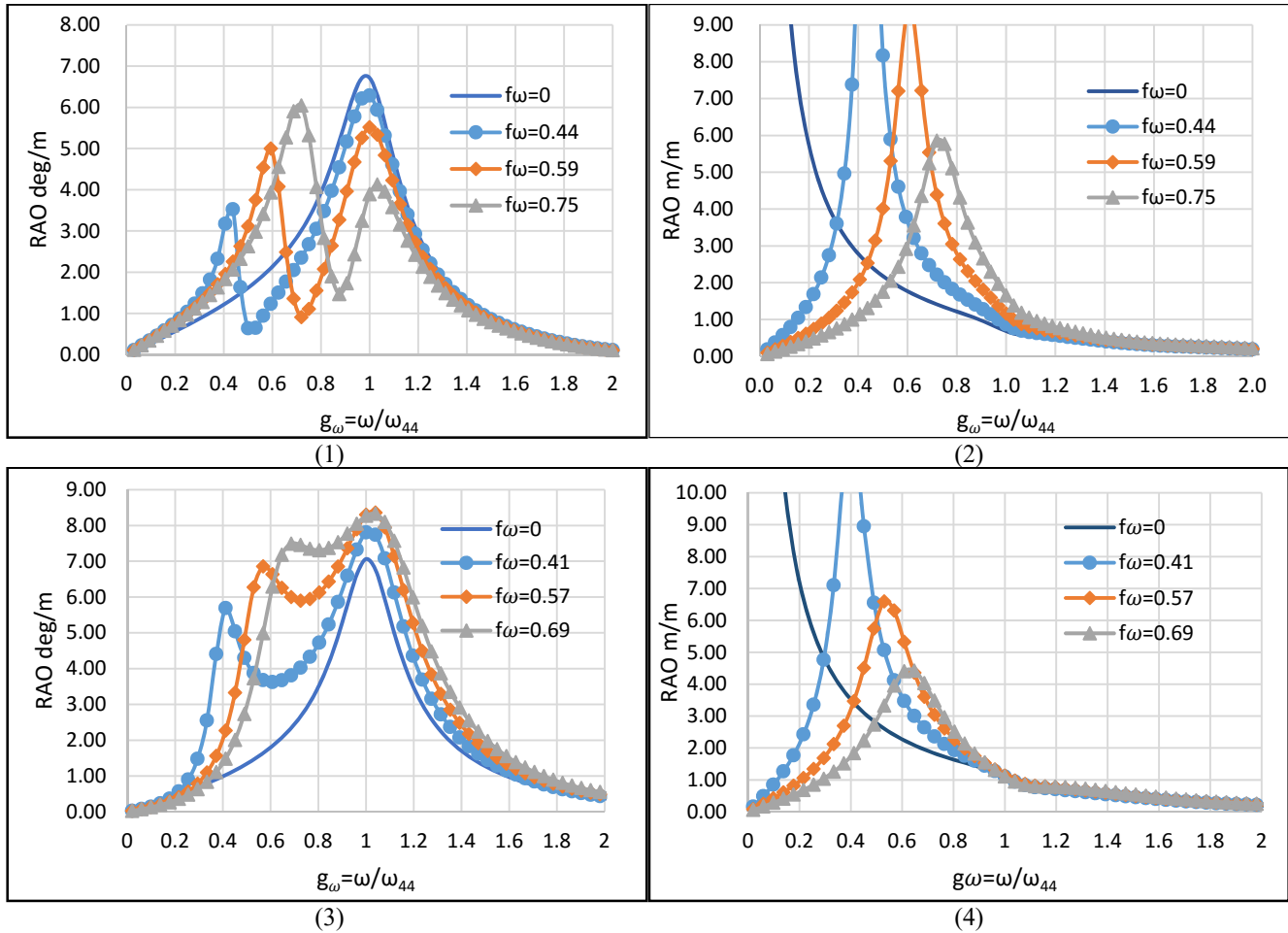


Figure 3.2 RAO of Fender-supported Tanks, (1) roll motion of empty tank; (2) sway motion of empty tank; (3) roll motion of full tank; (4) sway motion of full tank.

As seen from the figures above, compared with a free floating tank ($f_\omega=0$), tanks with fender supports have a very different responses. A soft fender can induce a resonant frequency on sway motion, while roll motion shows a two-peak response due to the coupling effect. The first roll peak response has the same frequency as sway, and the second one is almost the same as the free floating roll resonant frequency. For the empty tank, response of the original roll response peak (the maximum response at $f_\omega=0$) is reduced by the fenders, and this effect increases as the fender becomes stiffer. An opposite conclusion can be drawn from the responses of the full tank. Later an analysis of the motion equation will show that this is because of different VCG positions at different filling levels.

One prevailing property shown in the parametric study is that after adding the fender stiffness, the new roll RAO curves will intersect with the original curve of free floating tank. Thus the whole frequency domain is divided into two, one where the fender will increase the roll motion response, and one where it has the opposite effect. The relationship between the location of this intersection point and the fender properties will be discussed later in the selection of optimization criteria.

3.2 TIME DOMAIN NUMERICAL SIMULATION

Different from Hydrostar, in which fender effect can only be added to the tank by an external equivalent stiffness, the time-domain simulation software Orcaflex can model physical contact between fender and tank. Time-domain simulation is performed for two reasons: one is to check the validity of the frequency-domain model, and the other is to examine the tank response in irregular waves. Orcaflex model is shown below, with two fenders at each side of the tank. Two elastic blocks with higher stiffness are added in Y direction to prevent the tank from drifting away due to large translational motion.

Motion response with regular waves coming from 90 degree are simulated and compared with the frequency domain solution presented above. The natural frequency ratio $f_\omega = 0.75$, the same case shown in figure 3.2. The results are generally in good accordance, which proves the validity of the equivalent stiffness matrix. Differences may come from the impact between tank and fenders, which may induce nonlinear stiffness effects.

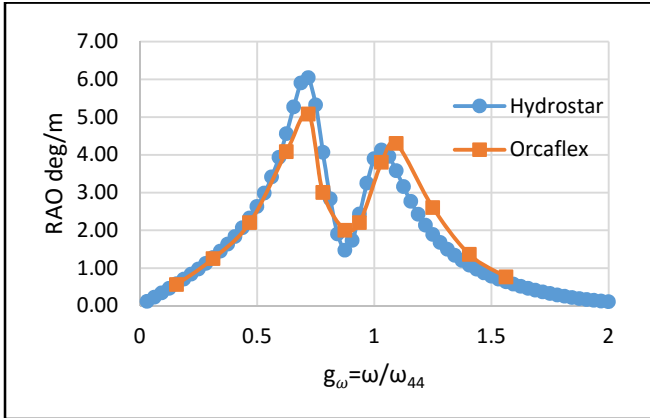


Figure 3.4 Comparison between Frequency and Time-domain Calculation Results

The random wave condition is defined by JONSWAP spectrum, with $H_s=1.8$ m, $T_p=7$ s, and $\gamma=3.3$. Even though they appear to be very mild, these are the prevailing extreme environment criteria for coastal areas near Singapore. The standard deviations of the motion and their respective maximum responses in a 3-hr random sea state are calculated and compared in Figure 3.5 and Figure 3.6 below. Similar to the frequency-domain responses, the fender effects on empty and fully loaded tanks are opposite. The relationship between motion statistics and natural frequency ratio is pictured below. It can be seen that sway motion generally declines when sway frequency increases. So increasing fender stiffness will bring benefit to both static and dynamic motion reduction. But maximum fender load will also be a concern. Roll motion shows different trends with empty and full tanks, similar as before. Also there are inflection points shown in the curves. For the empty tank, whose roll motion shows a decrease-increase shape, it means there's an optimized natural frequency ratio to minimize the rotation angle.

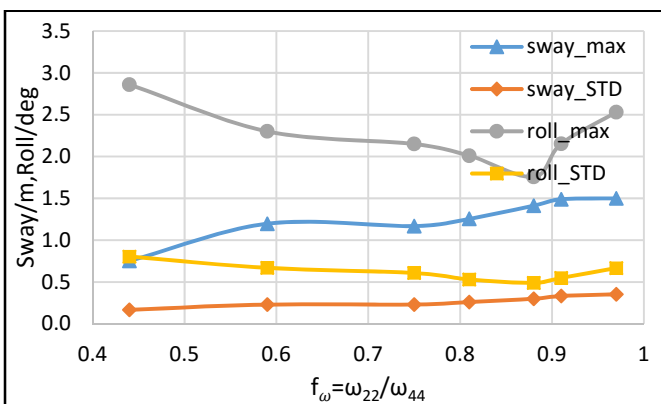


Figure 3.5 Maximum and RMS Motion Amplitude of Empty Tank

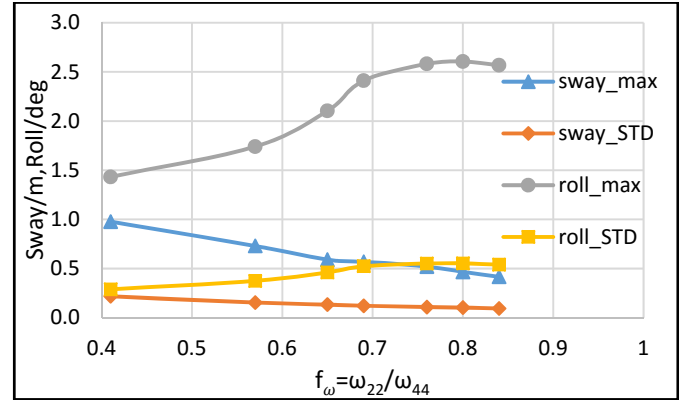


Figure 3.6 Maximum and RMS Motion Amplitude of Full Tank

4. OPTIMIZATION METHOD OF THE MARINE FENDER PARAMETERS

In this section the MDOF motion equations are simplified based on the hydrodynamic properties of the tank. So they are discussed first to justify the simplification of the equations.

First, for the tank with a large waterplane area, the hydrostatic stiffness of the roll/pitch motion is much larger than the fender stiffness, unless an unnecessarily stiff fender is used. So the existence of the normal fender stiffness K_{44} will not significantly modify the natural frequency of roll motion.

Besides, in this case resonance takes place at a low frequency, where diffraction is not severe, and the Froude-Krylov force is still the dominant wave excitation force component. This ensures that the wave force has a steady phase angle at the calculated frequency range. Hydrodynamic simulation shows that the wave force for sway motion has a phase angle of 0.5π and roll motion is 1.5π , which means the wave forces for these two DOFs are anti-phase. In order to simplify the argument, the wave excitation forces are first considered to have both constant amplitudes and phase angles. Later it can be seen that this simplification does not induce serious deviation of the results. The maximum wave force amplitude is used in following equations. The force amplitude is obtained from frequency domain calculation.

Finally, the added mass is neglected in the equation. For diagonal terms A_{22} and A_{44} , the error caused is negligible because of the mass ratio of the two DOFs. The coupling term A_{24} makes a difference, since it represents a coupling effect induced by the application point of wave excitation force. The effect of A_{24} can be tested by keeping $K_{24}=0$. In this case, however, since the applied fender stiffness is large enough to override this effect, neglecting A_{24} will only bring slight inaccuracy to the solution, which can be seen in section 4.2.

4.1 MDOF EQUATION OF FENDER COUPLING EFFECT

The undamped equation of motion of the coupled sway and roll motion is written as follows:

$$\begin{bmatrix} M_{22} & \\ & M_{44} \end{bmatrix} \begin{pmatrix} \ddot{x} \\ \ddot{\theta} \end{pmatrix} + \begin{bmatrix} K_{22} & K_{24} \\ K_{24} & K_{44} \end{bmatrix} \begin{pmatrix} x \\ \theta \end{pmatrix} = \begin{bmatrix} F_2 \cos \omega t \\ F_4 \cos(\omega t + \pi) \end{bmatrix} \quad (4.1)$$

Where M_{22} and M_{44} are the total mass of sway and roll degree, K_{22} is the fender normal stiffness equal to K , K_{24} is the coupling stiffness $K_{24} = Kd$, where d is the fender vertical position same as that in equation (2.1). F_2 and F_4 are the wave excitation forces treated as constant. The value is taken to be the maximum in the calculated frequency range. A phase lag of π is added to the wave excitation force F_4 for the reason stated previously.

The modal frequencies of the 2-DOF motion equation could be obtained by solving:

$$\det(Z) = \begin{vmatrix} K_{22} - M_{22}\omega^2 & K_{24} \\ K_{24} & K_{44} - M_{44}\omega^2 \end{vmatrix} = 0 \quad (4.2)$$

$$\left(\frac{\omega}{\omega_{44}}\right)^2 \left(\frac{\omega}{\omega_{22}}\right)^2 - \left[\left(\frac{\omega}{\omega_{44}}\right)^2 + \left(\frac{\omega}{\omega_{22}}\right)^2\right] + \left(1 - d^2 \frac{\omega_{22} M_{22}}{\omega_{44} M_{44}}\right) = 0 \quad (4.3)$$

Where $\omega_{22} = \sqrt{\frac{K_{22}}{M_{22}}}$, $\omega_{44} = \sqrt{\frac{K_{44}}{M_{44}}}$ is the uncoupled natural frequencies of sway and roll, $d = (Z_G - Z_S)$. The difference between modal frequencies of the MDOF system and the natural frequencies are determined by the mass ratio $M_{22}/M_{44} \approx r_g^2$ and the difference between the two natural frequencies, where r_g is the radius of gyration. For such a massive oil storage tanks, it is normal to have a gyration radius on the scale of 10m, which means the mass ratio is close to 0.01. As a result, the deviance of the resonant frequencies caused by coupling is determined by how close the two natural frequencies are, and the behavior of the coupled system can be divided into weak coupling (two natural frequencies are not close) and strong coupling cases.

The response amplitude with damping items could be written as:

$$\begin{pmatrix} A_2 \\ A_4 \end{pmatrix} = \begin{bmatrix} K_{22} + i\omega C_{22} - M_{22}\omega^2 & K_{24} \\ K_{24} & K_{44} + i\omega C_{44} - M_{44}\omega^2 \end{bmatrix}^{-1} \begin{bmatrix} F_2 \\ -F_4 \end{bmatrix} \quad (4.4)$$

$$= \frac{1}{\det(Z)} \begin{pmatrix} [M_{44}(\omega_{44}^2 - \omega^2) + i\omega C_{44}]F_2 + K_{24}F_4 \\ [-M_{22}(\omega_{22}^2 - \omega^2) + i\omega C_{22}]F_4 - K_{24}F_2 \end{pmatrix} \quad (4.5)$$

In which the first item of the right-hand side is the hydrodynamic force and the second item related to K_{24} is the coupling force item. The coupling effect will be determined by the signs of these two items. The overall response will be reduced if the two items have different signs and vice versa. This equation helps determine the fender effect under a regular design wave. If the marine structures are designed to have a lower natural frequency than design wave condition, $\omega_{design} > \omega_{44} > \omega_{22}$, the overall response decreases if $K_{24} > 0$. This effect will be more important if K_{24} has a larger amplitude. It should be noted that the empty and full tank studied in Section 3.1 have opposite VCG positions, and the equation (2.5) will explain the results in Figure 3.2.

The absolute fender effect should be obtained from comparison between the response of fender-supported tank and free floating tank (or soft mooring where sway and roll motion can be considered as uncoupled). From previous study we know that there's an intersection point between tank response curve

without fenders. This could be solved by making the SDOF and MDOF responses equal.

Rewrite the response of A_4 in the following way:

$$\left|\frac{A_4}{F_4}\right| = \sqrt{\frac{A^2 + B^2}{C^2 + D^2}} \quad (4.6)$$

Where

$$\begin{aligned} A &= K_{24} \frac{F_2}{F_4} + K_{22} - M_{22}\omega^2 \\ B &= \omega C_{44} \\ C &= (K_{22} - M_{22}\omega^2)(K_{44} - M_{44}\omega^2) - C_{22}C_{44}\omega^2 - K_{24}^2 \\ D &= C_{22}\omega(K_{44} - M_{44}\omega^2) + C_{44}\omega(K_{22} - M_{22}\omega^2) \end{aligned}$$

From the above equation, it is found the response amplitude is linked to: fender stiffness K , moment arm d , and the two viscous damping ratios, ζ_{22} and ζ_{44} . In the primary design when the damping effect is taken based on experience, these two parameters can bring uncertainty to the prediction of the fender effect. However, a sensitivity study shows that different damping ratios do not cause drastic change in the intersection frequency, which guaranteed the accuracy of the estimation on this key parameter. Furthermore, it means that the intersection point can be derived by setting both damping ratios equal to 0. The figure 3.7 shows curves of transmissibility magnitude $|A_4/F_4|$ vs wave frequency ratio with different damping applied. It is easily found out that the intersection point location of SDOF and MDOF curves is not sensitive to damping.

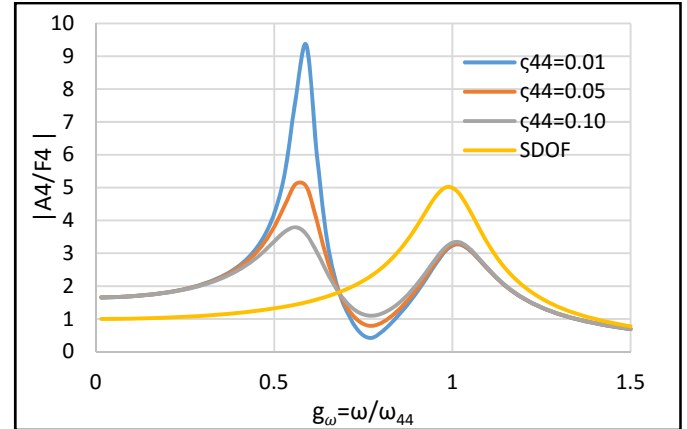


Figure 3.7 Sensitivity study on damping ratio

The x coordinate of the intersection point (hereinafter the intersection frequency) is given by setting the SDOF and MDOF responses equal:

$$\begin{aligned} \left|\frac{A_4}{F_4}\right| &= \left|\frac{1}{M_{44}(\omega_{44}^2 - \omega^2)}\right| \\ &= \left|\frac{\frac{F_2}{F_4} K_{24} + M_{22}(\omega_{22}^2 - \omega^2)}{M_{22}M_{44}(\omega_{22}^2 - \omega^2)(\omega_{44}^2 - \omega^2) - K_{24}^2}\right| \quad (4.7) \end{aligned}$$

In dimensionless form:

$$\left| \frac{1}{1 - g_{\omega}^2} \right| = \left| \frac{d f_r f_{\omega}^2 + f_{\omega}^2 - g_{\omega}^2}{(f_{\omega}^2 - g_{\omega}^2)(1 - g_{\omega}^2) - \mu d^2 f_{\omega}^4} \right| \quad (4.8)$$

Neglecting the item with the mass ratio, and the effective solution will be:

$$g_{inter} = \sqrt{1 + \frac{f_r d}{2} f_{\omega}} \quad (4.9)$$

Where $f_r = F_2/F_4$ is the excitation force ratio representing the relative strength between the environmental force input of the two DOFs.

The intersection frequency is determined eventually by the fender stiffness K , the supporting point position d and the relative amplitude of the excitation forces of the two DOFs, f_r .

4.2 VERIFICATION OF ANALYTICAL SOLUTION

The accuracy of the analytical solution given by equation (4.9) has to be checked against numerical simulation results. By restudying the case in Section 3.1, we can compare the intersection frequency from Hydrostar simulation and from calculation using the above equation. The comparison is listed in the tables below, and two more natural frequency ratios that are not shown in figure (3.2) are also used. It can be seen that the prediction is accurate adequate for initial design. It's worth noting that due to a very low VCG position for the fully-loaded tank, the intersection frequencies are very low, which means in a large frequency range, the fender is amplifying the roll angle. Figure (3.2) can be quoted as evidence to this point. One interesting finding is that for $d > 0$, the calculated intersection frequencies are mostly lower than those from numerical simulation, while for $d < 0$ it's the opposite. This is related to the neglected added mass terms. The neglected added mass becomes more important when draft is deep and there's only small gap between tank bottom and seabed.

Table 4.1 Comparison between simulation and analytical results, empty tank case ($f_r=0.20$)

f_{ω}	0.44	0.59	0.75	0.88	0.91
$g_{inter}/\text{Hydrostar}$	0.50	0.69	0.81	0.91	1.03
$g_{inter}/\text{calculated}$	0.47	0.64	0.81	0.87	0.95

Table 4.2 Comparison between simulation and analytical results, full tank case ($f_r=0.19$)

f_{ω}	0.41	0.57	0.65	0.69	0.8
$g_{inter}/\text{Hydrostar}$	0.20	0.28	0.32	0.35	0.41
$g_{inter}/\text{calculated}$	0.22	0.31	0.35	0.37	0.43

4.3 OPTIMIZATION CRITERIA OF MARINE FENDER SELECTION UNDER JONSWAP SEA STATE

From previous section we know the intersection frequency is the boundary between positive coupling and negative

coupling area. When $d > 0$, lower than this frequency the translational motion will excite the rotational motion while it would cancel part of the rotational motion. To achieve a positive d , the fender supporting point has to be below VCG of the tank. In reality this configuration is hard to accomplish, and will increase the damage from static loading. An alternative way will be placing multiple fenders vertically, so that when the tank is empty and has a shallow draft, only one set of the fenders will support it. When it sinks deeper into the sea due to heavy cargo loading, the deeper fender set will come into effect. The concept is illustrated below.

The equivalent fender stiffness and supporting point will be decided by the aggregated force acting on the tank. By changing the stiffness of the upper and lower fender layers, the equivalent fender stiffness K and moment arm d can be controlled.

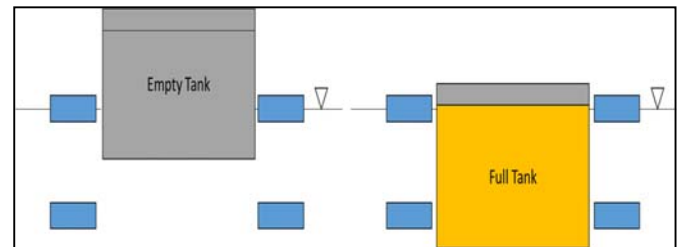


Figure 4.1 Concept of Double Layer Fender

The next question to be discussed will be how to select K and d . The JONSWAP spectrum in time domain simulation is used here as environmental input. The motion RAO and wave spectrum are drawn in the same diagram in figure (4.2.2), with their amplitude normalized for better view. The tank is already designed to have a resonant frequency with a sufficient distance with T_p , which is necessary in case the fender breaks down. The roll motion response is determined by the overlapped area of the motion response and wave spectrum in the wave frequency ratio range $g_{\omega} = [0.88, 2.5]$. The curve $f_{\omega}=0.81$ has an intersection frequency g_{inter} smaller than 0.88, which means in the whole wave energy zone roll RAO is reduced by fenders. So both maximum and significant roll motion responses are smaller than free floating tank. When f is increased to 0.87, the intersection point moves to $g_{inter}=0.97$, thus making the motion response higher in the energy zone from 0.88 to 0.97. In this case the significant motion response is still reduced, but on the contrary, the extreme value increases. This explains the decrease-increase tendency of the maximum response shown in section 3.2.

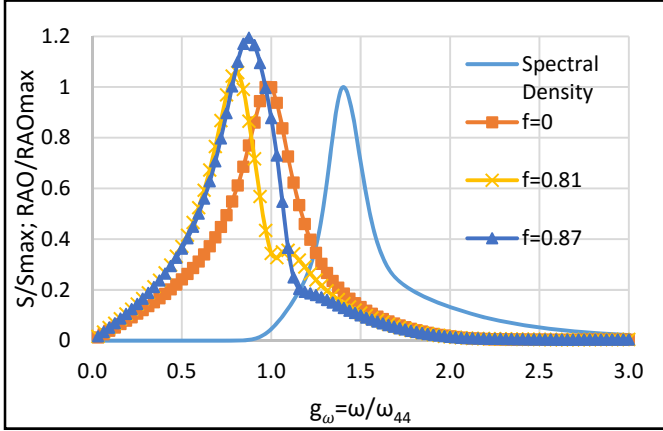


Figure 4.2 RAO Optimization against JONSWAP Spectrum

As a result, to make sure the fender is beneficial to the roll motion reduction, it's necessary to keep intersection frequency out of wave energy zone. By taking other constraints into consideration, the fender selection steps could be summarized as the following:

- (1) The lower bound of the fender stiffness K_{\min} should be sufficient to:
 - constrain maximum tank displacement (or maximum fender deformation) in a satisfactory range. This displacement can be initially seen as the superposition of static and dynamic motion responses. Static displacement will be estimated from constant fender stiffness K and static environmental force from current and wind. The dynamic component can be obtained by RAO calculation like that shown in section 3.1.
 - Avoid energy concentrated at frequencies of first-order excitation forces.
- (2) The upper bound of the fender stiffness K_{\max} will be initially determined by maximum contact force the tank and fender could withstand. Contact force could be estimated by the maximum displacement of the tank multiplied by fender stiffness, but impact weighs more when there's a gap between tank and fenders, or fender stiffness is large. So a time-domain simulation can be used to verify the initial estimate.
- (3) If the range determined from (1) and (2) is still wide, the fender stiffness K_{\max} can be further limited by keeping g_{inter} smaller than the lower bound of JONSWAP spectrum where wave energy is negligible. If the fender configuration is fixed, thus the moment arm d is positive but cannot be changed, an applicable fender stiffness will be obtained by keeping them equal:

$$g_{\text{inter}} = \text{Min}[g_{S>0}] \quad (4.1)$$

If d is negative, fender will exaggerate the roll motion response when $g > g_{\text{inter}}$. This effect should be minimized, and K should be taken at the lower bound.

- (4) The fender effect on the roll motions should be checked at all filling levels and should be taken into consideration in the initial motion check.

The fender effect on RMS motion can also be estimated from the relation between motion spectrum and wave spectrum as follows:

$$S_M(\omega) = \text{RAO}^2 S_w(\omega) \quad (4.2)$$

The reduced zeroth order moment of the motion spectrum can be estimated by:

$$\Delta m_0 = (\text{RAO}^2 - \text{RAO}_f^2) S_w(\omega) \quad (4.3)$$

In which RAO and RAO_f are the motion responses with and without fender.

5. A PARAMETRIC STUDY OF MARINE FENDER EFFECT ON PARTIALLY FILLED TANK

Up to this point, the effects of the internal liquid has been included only through its solid mass. Partially filled tanks are frequently encountered in daily operation. When there is a free surface inside the tank, sloshing will take place under wave excitation, and at certain filling levels it alters the motion response of the tanks significantly. In frequency domain method, the sloshing effect on tank motion is treated as frequency-dependent added mass and damping items, [5]. When tank is free floating, the sloshing-induced added mass and tank roll responses are illustrated below in Figure 5.1. The wave frequency ratio g in the x axis is still calculated using resonant frequency of the empty tank. The motion RAO indicates a clear 2 DOF response property, which implies that the sloshing has a similar effect as introducing a new DOF into the system. The analytical expression of sloshing-induced added mass is another evidence for this hypothesis, [6]. If the partially filled tank is supported by fenders, the three DOFs will be coupled together.

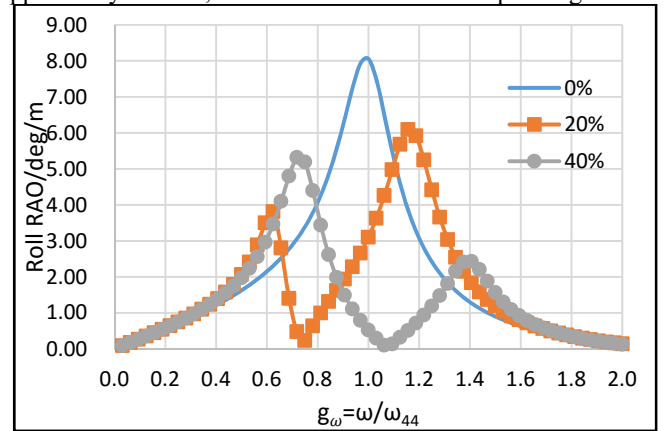


Figure 5.1 Roll Motion RAO of Partially-Filled Free Floating Tank

A parametric study on the 40% filled tank has been carried out to investigate on the fender effect on partially filled tank. The tank has a VCG = -3.704 m. Damping ratio on sway and roll is still assumed to be 10%, and a damping coefficient of 0.01 is applied to sloshing as a default in Hydrostar calculation (ref). A

variety of fender stiffness K and moment arm d is applied. The results show that sway is still not much influenced by sloshing, sway responses are not shown for sake of conciseness. Figure 5.2 shows the sensitivity study of fender stiffness K with single fender layer located at water level ($d = -3.704$ m), and figure 5.3 shows the effect of controlling moment arm d when keeping K constant ($f_{\omega} = 0.47$). It can be seen that when sway natural frequency is low, fender has a limited effect on the motion near sloshing peak frequency. Most of the fender effect is still concentrated near the low frequency peak near $g_{\omega} = 0.7$. To conclude, the fender has a limited effect on sloshing. The good side of the conclusion is that we can study the empty and fully-loaded tank cases to select the fenders, and double check the motion with sloshing after selection.

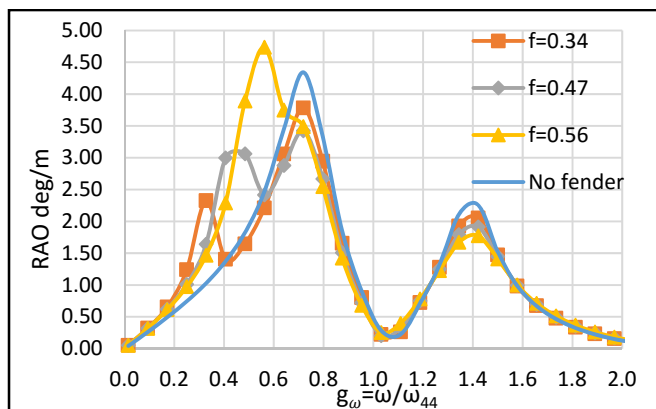


Figure 5.2 Roll RAO Sensitivity Study on Fender Stiffness

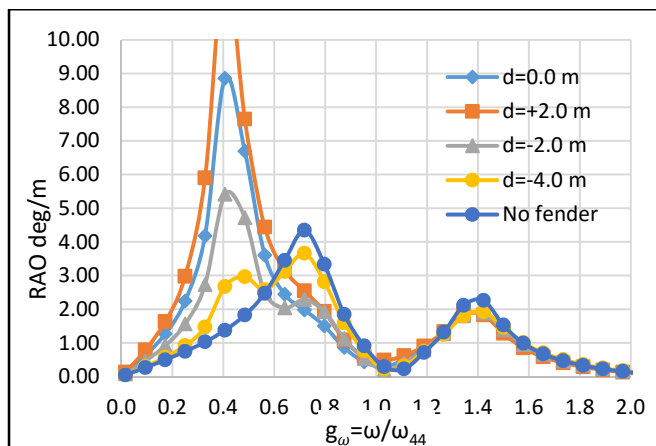


Figure 5.3 Roll RAO Sensitivity Study on Fender Moment Arm

6. CONCLUSION AND FUTURE WORK

This paper is a summary of the effort on trying to optimize the marine fenders that are part of the permanent mooring system of a floating oil storage tank. The optimization goal is to control the

lateral motion, rotational motion modified by coupling effect, maximum displacement and contact force. The numerical simulation shows that the fender induced translational and rotational movements under wave excitation behave like a multi DOF rigid body motion with strong coupling effect. The comparison between analytical and numerical results show that regardless of the frequency dependent added mass and excitation force, the tank motion RAO is still highly predictable using simple multi DOF motion equations, on condition that the wave diffraction effect is relatively small. Essentially it means that long wave is encountered and wave exciting force is largely dominated by the F-K force, thus a stable phase angle of the wave excitation force is expected. Besides, the prediction method inherits all the limitations of the linear potential flow theory. The purpose of bringing up the simple model is firstly to interpret the frequency domain calculation results and save time for the repetitive trial runs of the software, trying to get the best solution of the marine fender parameters. In section 4.3 a simple way of estimating fender effect on RMS motion in random sea state is proposed and can be used for reducing repetitive modelling and simulating work load or estimating tank behavior in irregular waves without resorting to a time-domain simulation tool.

One of the main future tasks is to verify the frequency domain calculation and the optimization criteria using model tests. This is also true for the assumed roll damping of 10% of critical. Once validated, the selection of marine fender can be integrated into the initial sizing study for the new concept design. More detailed guideline on fender selection can also be proposed for more general design problems.

ACKNOWLEDGEMENT

The authors wish to thank the Land and Livability National Innovation Challenge (L2NIC) for their support and JTC Corporation for their permission to publish this work. The views expressed herein are the sole opinions of the authors and may differ from those of the sponsors. Also, support from Orcina for the kind permission to use their Orcaflex software and to Bureau Veritas for the Hydrostar license are gratefully acknowledged.

REFERENCES

- [1] PIANC Guidelines for the design of fender systems, 2002.
- [2] Den Hartog, Jacob Pieter, Mechanical Vibration, New York, McGraw-Hill, 1956.
- [3] BV, HYDROSTAR user manual ver. 7.25, 2014
- [4] Orcina, OrcaFlex Manual ver. 10.0a, Orcina Ltd, Ulverston, Cumbria, 2015.
- [5] Malenica S., Zalar M. and Chen XB., Dynamic coupling of seakeeping and sloshing, Proceedings of the International Offshore and Polar Engineering Conference, 2003.
- [6] Faltinsen O.M., Sloshing, New York, NY : Cambridge University Press, 2009.